

Human ZMPSTE24 disease mutations: residual proteolytic activity correlates with disease severity

Jemima Barrowman¹, Patricia A. Wiley², Sarah E. Hudon-Miller², Christine A. Hrycyna² and Susan Michaelis^{1,*}

¹Department of Cell Biology, The Johns Hopkins School of Medicine, Baltimore, MD 21205, USA and ²Department of Chemistry, Purdue University, West Lafayette, IN 47907, USA

Received April 7, 2012; Revised May 30, 2012; Accepted June 11, 2012

The zinc metalloprotease ZMPSTE24 plays a critical role in nuclear lamin biology by cleaving the prenylated and carboxylmethylated 15-amino acid tail from the C-terminus of prelamin A to yield mature lamin A. A defect in this proteolytic event, caused by a mutation in the lamin A gene (*LMNA*) that eliminates the ZMPSTE24 cleavage site, underlies the premature aging disease Hutchinson-Gilford Progeria Syndrome (HGPS). Likewise, mutations in the *ZMPSTE24* gene that result in decreased enzyme function cause a spectrum of diseases that share certain features of premature aging. Twenty human *ZMPSTE24* alleles have been identified that are associated with three disease categories of increasing severity: mandibuloacral dysplasia type B (MAD-B), severe progeria (atypical 'HGPS') and restrictive dermopathy (RD). To determine whether a correlation exists between decreasing ZMPSTE24 protease activity and increasing disease severity, we expressed mutant alleles of *ZMPSTE24* in yeast and optimized *in vivo* yeast mating assays to directly compare the activity of alleles associated with each disease category. We also measured the activity of yeast crude membranes containing the ZMPSTE24 mutant proteins *in vitro*. We determined that, in general, the residual activity of *ZMPSTE24* patient alleles correlates with disease severity. Complete loss-of-function alleles are associated with RD, whereas retention of partial, measureable activity results in MAD-B or severe progeria. Importantly, our assays can discriminate small differences in activity among the mutants, confirming that the methods presented here will be useful for characterizing any new *ZMPSTE24* mutations that are discovered.

INTRODUCTION

ZMPSTE24 is a zinc metalloprotease required for the maturation of the nuclear scaffold protein, lamin A (1–4). Lamin A, together with lamin C and the B-type lamin proteins, form the meshwork that underlies the nuclear envelope. Lamins provide structure and shape to the nucleus, and play many critical roles in nuclear function. These roles include, but are not limited to, binding of heterochromatin, regulation of transcription factors, positioning of nuclear pore complexes and facilitation of the DNA damage response (5–8).

Lamin A and the B-type lamins are synthesized as precursors that terminate in a CAAX motif (where C is cysteine, A is often an aliphatic amino acid and X is any residue). CAAX proteins are post-translationally modified in a series of ordered reactions beginning with farnesylation of the

CAAX cysteine, followed by endoproteolytic removal of the terminal AAX residues, and ending with carboxylmethylation of the terminal farnesyl-cysteine (Supplementary Material, Fig. S1 (right), steps 1–3) (4,9). For reasons that are not fully understood, the lamin A precursor protein, called prelamin A, undergoes a surprising additional step in which the 15-amino acid modified tail is removed, resulting in mature lamin A that does not retain the hydrophobic modifications (Supplementary Material, Fig. S1 (right), step 4) (10–13). In contrast, B-type lamins do not undergo this final cleavage event, and retain their lipid-modified and carboxylmethylated tail (5). Lamin C, a short A-type lamin splice isoform generated from the *LMNA* gene, lacks the CAAX motif altogether and thus does not undergo post-translational modification. The zinc metalloprotease ZMPSTE24 mediates the last cleavage step in the lamin A maturation pathway (1–4).

*To whom correspondence should be addressed. Email: michaelis@jhmi.edu

ZMPSTE24 is a membrane-associated enzyme that is predicted to contain seven transmembrane segments and is localized to the ER membrane and the inner nuclear membrane (14,15). ZMPSTE24 contains a consensus zinc metalloprotease motif, consisting of a HEXXH catalytic site, located in a loop predicted to reside in the cytosol/nucleoplasm (1,16,17). Farnesylated substrates such as prelamin A are accessible to the HEXXH domain for proteolytic cleavage.

The failure to cleave the farnesylated and carboxylmethylated tail from the prelamin A precursor due to *LMNA* mutations that remove the ZMPSTE24 cleavage site can severely impact human health and longevity. For example, the classical premature aging disease, Hutchinson-Gilford Progeria Syndrome (HGPS), is most commonly caused by a dominant mutation (c. 1824C>T; p. G608G) in *LMNA* that activates a cryptic mRNA splice site and leads to an internal in-frame deletion of 50 amino acids that removes the ZMPSTE24 cleavage site within prelamin A (18,19). The resulting mutant lamin A protein (called progerin) cannot be cleaved. HGPS is a childhood disease characterized by an onset of premature aging symptoms by age 2 years that include loss of hair, thin skin and progressive cardiovascular disease from which the children succumb at an average age of 13 years (20,21). Two significantly more severe cases of HGPS have been documented in which alternative mutations (c. 1968+1G>A and c. 1821G>A) serve as more potent activators of the cryptic splice site, and result in the generation of more progerin and death at an earlier age (22). Retention of the hydrophobic farnesyl and carboxylmethyl modifications disrupts the normal function of lamin A (and/or allows it to acquire a new function), conferring a dominant-negative phenotype. The amount of toxic progerin in cells appears to correlate with the severity of disease outcomes (22). In a mouse progeria model, preventing progerin farnesylation by genetic alteration of the progerin CAAX motif or treatment with a farnesyltransferase inhibitor lessens disease phenotypes (23–25).

Mutations in *ZMPSTE24* are associated with diseases that share features of progeria. The aberrant form of prelamin A that results from decreased ZMPSTE24 activity permanently retains its farnesylated and carboxylmethylated tail, similar to progerin. The *zmpste24*^{-/-} mouse exhibits a severe progeroid disorder that is completely alleviated in a mouse heterozygous for lamin A (*zmpste24*^{-/-} *lmna*^{+/-}), which reduces the load of toxic prelamin A by 50%. Thus, the amount of uncleaved, persistently prenylated prelamin A is thought to be the critical determinant of disease phenotypes (1,26–33).

Three distinct but related human diseases, with a gradation of severity, result from ZMPSTE24 mutations. These include, in order of increasing severity, the relatively mild disorder mandibuloacral dysplasia (MAD-B) (27–29,32,34–37), a severe form of progeria [sometimes called atypical HGPS and here designated AT ‘HGPS’ (33,38)], and the lethal neonatal disease restrictive dermopathy (RD) (29,30,39–44). These diseases are termed progeroid disorders because they share features in common with HGPS, such as thin skin (RD), lipodystrophy (MAD-B) and premature aging (AT ‘HGPS’) (27,29,33,38,43). The inheritance pattern of these diseases is autosomal recessive; thus, both chromosomal *ZMPSTE24* copies are defective (29,43). It should be noted that an early report concluding that RD is digenic (45) was

later corrected (29,43). Heterozygous carriers of disease alleles are unaffected. Thus, a single functional copy of *ZMPSTE24* is sufficient to prevent disease (28–30,37,40).

Several of the *ZMPSTE24* mutations that cause MAD-B have previously been assayed for activity using a qualitative yeast-based *in vivo* halo assay (27,28,46). However, a direct side-by-side comparison between the various human *ZMPSTE24* disease mutations identified to date has not been performed, nor have any quantitative methods been used to assay these alleles. Herein we have utilized *in vivo* and *in vitro* yeast halo, mating and activity assays to quantitate and directly compare the activities of a panel of *ZMPSTE24* disease mutants associated with each disease category (MAD-B, AT ‘HGPS’ and RD). We also examined a newly reported *ZMPSTE24* allele potentially associated with metabolic syndrome (47). Using these assays, we demonstrate that mutant alleles associated with RD have no activity, while *ZMPSTE24* alleles associated with MAD-B or AT ‘HGPS’ retain residual activity. Thus, ZMPSTE24 activity can be correlated to the severity of the disease state. Importantly, we report conditions using established activity assays that are able to reveal small differences in enzymatic activity. These assays will be useful for analyzing newly discovered mutations in *ZMPSTE24*.

RESULTS

Nineteen patients with homozygous or compound heterozygous mutations in *ZMPSTE24* have been reported in the literature. These individuals have been diagnosed with MAD-B, AT HGPS or RD, as indicated (Fig. 1). In RD patients (Fig. 1, lines 10–19), both *ZMPSTE24* mutations might reasonably be expected to represent ‘null’ alleles that cause complete loss of protein function. These include frameshift or nonsense mutations that cause early termination, or large internal in-frame deletions that could interfere with the membrane topology of ZMPSTE24. In contrast, MAD-B or AT ‘HGPS’ patients (Fig. 1, lines 1–8) generally have a predicted null allele in combination with a point mutation (or two point mutant alleles) that could potentially partially affect, but not eliminate, ZMPSTE24 enzymatic activity.

Our goal in this study was to quantitatively assess enzymatic activity across the spectrum of *ZMPSTE24* alleles to determine whether the level of residual proteolytic activity, or lack thereof, correlates with disease severity. The individual disease mutants we examined in this study are highlighted in yellow in Figure 1. These include the substitution mutations P248L, W340R and N265S that result in MAD-B or AT ‘HGPS’ when present in combination with a possible null allele (such as W450X or L362F(fsX18), also tested herein) (Fig. 1, lines 1–4, 6 and 8), and L94P that causes MAD-B when homozygous (Fig. 1, line 5). We also tested the homozygous in-frame deletion mutation T159_L209del identified in a case of RD (Fig. 1, line 16). Taken together, the alleles we investigated in this study (including substitutions, frameshifts, internal in-frame deletions and null alleles) represent mutant ZMPSTE24 proteins that retain the catalytic zinc metalloprotease HEXXH motif at position 335–339 (Fig. 2 and Supplementary Material, Fig. S2). Additional mutants that are

Disease	ZMPSTE24 Mutations		Reference
	Partial	Null/Partial	
1) MAD	P248L	Q41X	Miyoshi et al., 2008
2) MAD	P248L	W450X	Ahmad et al., 2010
3) MAD	W340R	L362F(fsX18)	Agarwal, 2003 Moulson et al., 2005
4) MAD	N265S	Y70S(fsX3)	Cunningham et al., 2010
5) MAD	L94P	L94P	Ben Yaou et al., 2011
6) MAD	N265S	L362F(fsX18)	Agarwal et al., 2006
7) MAD	L462R	unidentified	Thill et al., 2008
	Null/Partial	Null/Partial	
8) AT "HGPS"	N265S	L362F(fsX18)	Shackleton et al., 2005
9) AT "HGPS"	V402S(fsX1)	V402S(fsX1)	Denecke et al., 2006
	Null	Null	
10) RD	L362F(fsX18)	L362F(fsX18)	Morais et al., 2008 Navarro et al., 2005 Kariminejad et al., 2009
11) RD	I19Y(fsX28)	I19Y(fsX28)	Moulson et al., 2005
12) RD	I198Y(fsX19)	I198Y(fsX19)	Moulson et al., 2005
13) RD	L91_L209del	L362F(fsX18)	Navarro et al., 2005
14) RD	P99L(fsX38)	L362F(fsX18)	Navarro et al., 2005
15) RD	Q417X	L362F(fsX18)	Navarro et al., 2005
16) RD	T159_L209del	T159_L209del	Sander et al., 2008
17) RD	K17S(fsX21)	Y195F(fsX22)	Smigiel et al., 2010
18) RD	E239X	E239X	Chen et al., 2009
19) RD	E231X	E231X	Jagadeesh et al., 2009
	Severe truncations: mutants do not retain catalytic domain	TESTED IN THIS STUDY: mutants retain catalytic domain	

Figure 1. Summary of the *ZMPSTE24* disease alleles reported in cases of MAD, atypical HGPS and RD. Diseases are grouped in order of increasing severity, with MAD-B as the least severe and RD as most severe. The pairwise combination of specific mutations that have been attributed to each patient case is provided. Grey shading indicates mutants that do not retain the domain containing the HEXXH motif, which lies in positions 335–339 in *ZMPSTE24*. Mutants tested in this study are highlighted in yellow.

predicted to retain the catalytic domain (L462R, V402S(fsX1), L91_L209del, Q417X; Fig. 1, lines 7, 9, 13, 15) were not examined here; however, Q417X and V402S(fsX1) have been previously reported to lack activity by using either a yeast-based activity assay (V402S(fsX1)) or by examination of prelamin A processing (Q417X) (38,43).

The positions of the amino acid residues that are altered or the segments that are deleted by the *ZMPSTE24* mutations tested here are schematized in Figure 2. In addition to the mutants highlighted in yellow in Figure 1, we also included a recently identified *ZMPSTE24* mutation (L438F) that was detected in a patient with metabolic syndrome (47). This mutation represents an unusual case, as a second allelic mutation was not detected in the patient, a finding that seemingly contradicts the autosomal recessive nature of diseases associated with *ZMPSTE24* mutations. Nevertheless, because L438F may be implicated in disease and may also provide useful

structure–function information, we included this mutation in our studies.

***In vivo* a-factor halo assays can broadly distinguish active versus inactive *ZMPSTE24* disease alleles**

The yeast homolog of *ZMPSTE24* is *STE24*, which is critical for the production of the *Saccharomyces cerevisiae* mating pheromone, a-factor (Supplementary Material, Fig. S1, left) (48). The Ste24 protein plays a redundant role with Rce1 in the proteolysis of the C-terminal three amino acids of the CAAX motif; Ste24 also performs a unique role in an N-terminal cleavage event required to produce mature, bioactive a-factor, similar to the role of *ZMPSTE24* in lamin A processing (Supplementary Material, Fig. S1) (4,16,17, 48–53). Importantly, the mammalian homologue of *STE24*, *ZMPSTE24*, can complement both of these Ste24 activities

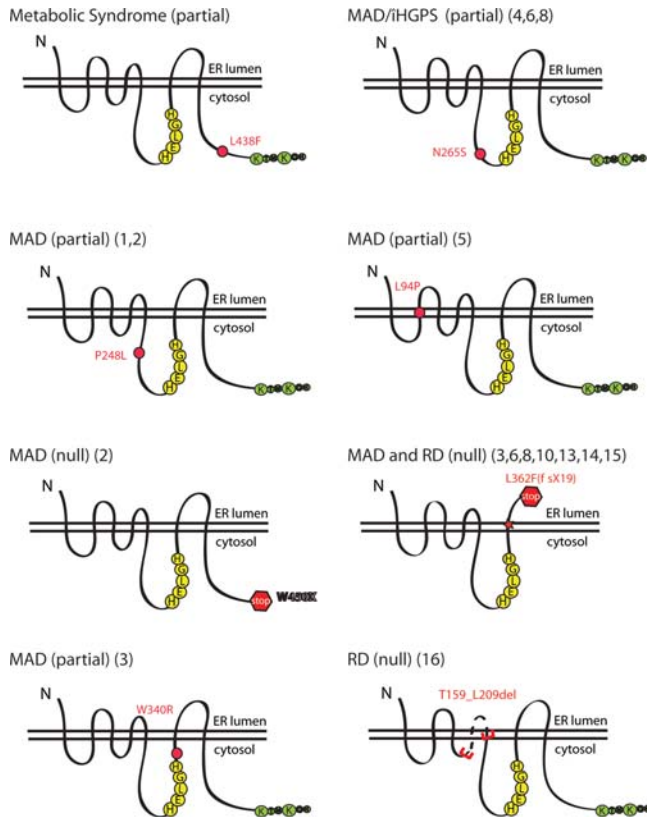


Figure 2. Schematic of the patient mutations analyzed in this study by *in vivo* and *in vitro* activity assays. ZMPSTE24 is predicted to contain seven transmembrane spans, with three cytosolic loops and a C-terminal cytosolic tail containing a dilysine ER retrieval motif (green). The loops are drawn roughly to scale. Representative schematics show the approximate location of the molecular lesions in the ZMPSTE24 mutants examined in this study. The HEXXH catalytic motif (HELGH) in human ZMPSTE24 is at positions 335–339 (yellow). The correlation to the disease/patient case as shown in Figure 1 is noted in parentheses.

in a-factor biogenesis, as the heterologous expression of human ZMPSTE24 in a *ste24Δ rce1Δ* double mutant can restore export of a-factor (16). The a-factor exported from cells of the *MAT α* mating type binds to receptors on cells of the opposite mating type (*MAT α*) and stimulates mating. Thus, mating efficiency can be used as an indirect measure of Ste24/ZMPSTE24 activity (49,54). An alignment of the yeast and human enzymes is shown in Supplementary Material, Figure S2.

Initially, we used the well-established qualitative yeast-based halo assay to systematically compare the export of biologically active a-factor from the yeast strain SM3614 (*MAT α ste24Δ rce1Δ*) expressing each ZMPSTE24 allele predicted to retain the HEXXH catalytic motif on a *CEN URA3* plasmid (Fig. 3A). The halo assay has previously been used to qualitatively assess a few ZMPSTE24 disease alleles for activity (27,28,34); however, multiple side-by-side comparisons of a series of ZMPSTE24 alleles have not been performed with this assay. As a control for catalytically inactive ZMPSTE24, we included a mutation (H335A) in the histidine residue of the HEXXH catalytic motif. This mutation is predicted to eliminate activity, based on the evidence from yeast Ste24 HEXXH mutations (H297A, E298A and

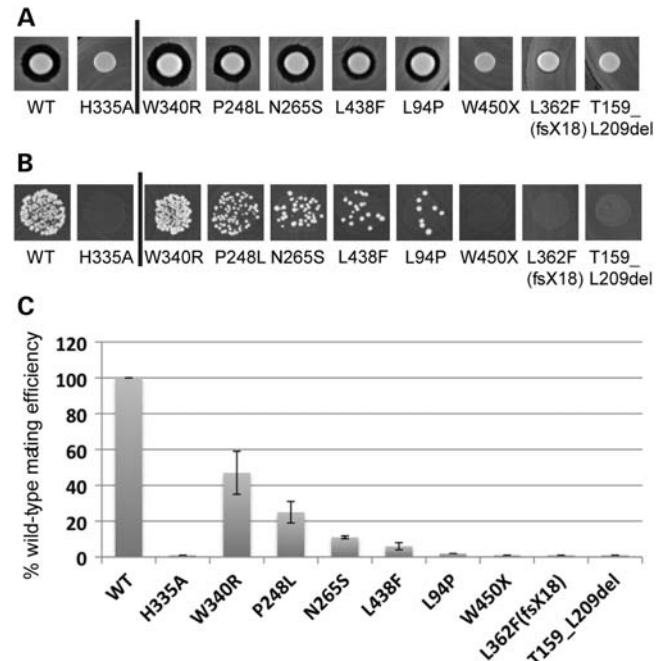


Figure 3. The halo and mating assays reveal measurable differences in activity of ZMPSTE24 mutants. Results of the qualitative halo assay (A) and the plate mating assay (B) are shown. Results of a quantitative filter mating assay are graphically represented below (C). The details of how these tests were performed are discussed in the text. The mating percentages graphed in (C) are normalized to WT (100%). The values for each mutant tested were: H335A (1%), W340R (47%), P248L (25%), N265S (11%), L438F (6%), L94P (2%), W450X (1%), L362F(fsX18) (1%) and T159_L209del (1%).

E298D), in which mating activity is completely lacking (48). For the halo assay, the *MAT α* cells expressing ZMPSTE24 are spotted onto a lawn of tester cells of the opposite mating type (*MAT α*) containing a mutation (*sst2*). The ‘supersensitizing’ *sst2* mutation causes irreversible cell cycle arrest and thus death of cells in the lawn that come in contact with secreted a-factor (51). As a result, the diffusion of the secreted bioactive a-factor away from a spot of *MAT α* cells results in a circular ‘kill zone’ in the underlying *MAT α sst2* lawn that is indicative of a-factor activity.

As evident in Figure 3A, cells expressing wild-type ZMPSTE24 produce an a-factor halo, as expected, whereas cells expressing the H335A mutation, presumed to be important for catalytic activity, do not. Thus, the HEXXH motif is indeed critical for activity of human ZMPSTE24 (Fig. 3A, left, and results below), just as it is for yeast STE24 (48). Interestingly, five ZMPSTE24 alleles to the right of the bar (W340R, P248L, N265S, L438F and L94P) all produce an a-factor halo, which is indicative of at least some ZMPSTE24 activity, whereas a halo is lacking for the other alleles (W450X, L362F(fsX18), and T159_L209del). It is apparent that the a-factor halo assay is useful for discerning the differences between null (W450X, L362F(fsX18) and T159_L209del) and at least partially active alleles (W340R, P248L, N265S, L438F and L94P).

However, it is notable that small differences in activity between the point mutants or the wild-type protein are harder to discriminate and are not obvious using this halo assay. For instance, the W340R mutant cannot be

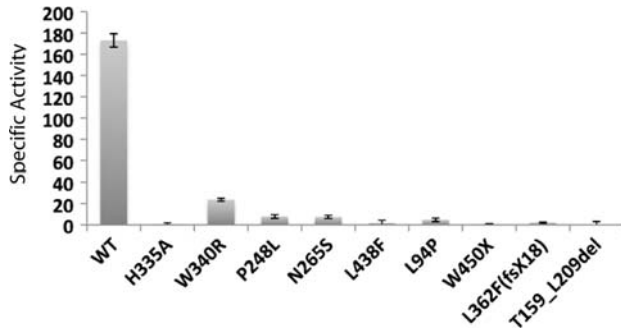


Figure 4. A coupled *in vitro* proteolysis activity assay reveals differences in specific activity for the *ZMPSTE24* disease mutants. The specific activity of membrane preparations containing wild-type *ZMPSTE24*, the H335A catalytic site mutant and disease mutants were determined by the coupled proteolysis and methylation assay described in the text. Experiments were performed three times in triplicate for each *ZMPSTE24* protein (for a total of nine trials).

distinguished from wild-type *ZMPSTE24*, but is indeed defective in activity, as shown below (Figs 3C and 4). Furthermore, P248L is indistinguishable from N265S, L438F and L94P in the halo assay, but shows significantly greater activity than the others in the more quantitative assays below. It should be noted that a very tiny halo is seen with the L362F(fsX18) mutant, and has previously been observed under conditions where a concentrated cell suspension was used (27). The mutation in this case results in a frameshift predicted to eliminate the entire C-terminus of *ZMPSTE24*. It is possible that the very low but detectable residual activity observed for this allele in the extremely sensitive α -factor halo assay may be due to a small amount of ‘read-through’ of the premature translational stop codon. Notably, almost no activity is detectable for this L362F(fsX18) allele by the quantitative assays (Figs 3C and 4) below.

***In vivo* mating assays reveal a range of activity differences associated with *ZMPSTE24* disease alleles**

The halo assay described above is hypersensitive, and gives a positive signal for any small residual activity. Due to this extreme sensitivity, the halo assay is not useful for the quantitation of low but measurable differences in enzyme activity that could result in significant differences in disease severity in humans. To refine and advance the methods that can be used to more quantitatively compare the biological activity of disease alleles of *ZMPSTE24*, we employed a yeast mating assay. Importantly, this assay can accurately reflect differences in α -factor export and can be modified, by varying the *MAT α* tester strains or assay conditions that are used, to obtain optimal sensitivity in the range of interest (49,54).

We expressed wild-type *ZMPSTE24* and each mutant allele on a plasmid in the *MAT α ste24 Δ rce1 Δ* strain SM3614, and assayed the ability of the strain to mate by spotting the strains onto a lawn of tester *MAT α* cells (Fig. 3B). To maximize our ability to discriminate the small but significant differences in activity of the *ZMPSTE24* mutants analyzed here, we utilized a ‘stringent’ mating condition that relies on a *MAT α* mating tester strain containing a *far1* mutation (55). The *far1* mutation lowers the efficiency of the mating response,

and confers a different range of sensitivity to the mating assay that is better suited to the mutants studied here than the standard assay using a wild-type *MAT α* mating tester strain that registers positive for any small amount of activity. In contrast, when *far1* cells were used as the tester strain, many of the *ZMPSTE24* mutant proteins tested here conferred a graded range of reduced mating efficiency compared with the wild-type (Fig. 3B). Importantly, small but significant differences in mating activity are revealed between the W340R, P248L, N265S, L438F and L94P substitution mutations.

To more accurately quantify the residual activities of the partially active alleles, we utilized a quantitative filter mating assay (Fig. 3C). For quantitative mating, strains are allowed to mate for a limited time (4 h) on a filter disc prior to plating on media selective for diploids. The number of diploids that form in proportion to the total number of cells provides a quantitative measure of mating efficiency (54,56). The results from the quantitative mating assay correlate well with our qualitative spot assay (compare Fig. 3C with B), and differences in mating efficiency can be reproducibly discerned for each of the point mutations in *ZMPSTE24*. W340R retains ~47% of wild-type activity, while P248L (25%), N265S (11%), L438F (6%) and L94P (2%) all show an even further reduction in activity. The premature termination, frameshift and deletion mutants, W450X, L362F(fsX18) and T159_L209del, respectively, register essentially no activity under these conditions. Notably, the spot-mating tests (Fig. 3B) and the quantitative mating test (Fig. 3C) provided similar information. Interestingly, the W340R mutant shows significantly higher residual activity in the mating assay (~50%) than the others.

Enzymatic activity of *ZMPSTE24* disease alleles

The activity of mammalian *ZMPSTE24* expressed in yeast can be determined *in vitro* using a well-established coupled assay (53,57–59). This coupled endoproteolysis and methylation assay indirectly measures the proteolysis of the C-terminal three amino acids of the CAAX motif (Supplementary Material, Fig. S1, step 2), by quantifying the resulting farnesyl-cysteine methyl esters that become available for carboxymethylation by isoprenyl cysteine carboxyl methyltransferase (ICMT), also called Ste14 in yeast (Supplementary Material, Fig. S1, step 3). In this assay, crude membranes prepared from the *ste24 Δ rce1 Δ* strain (SM3614), expressing wild-type or mutant *ZMPSTE24* alleles, are the source of enzyme. The membranes are incubated with the substrate, a synthetic farnesylated peptide containing an intact C-terminal CAAX motif. *ZMPSTE24* present in the membrane preparations endoproteolytically removes the terminal AAX residues, exposing the farnesylated cysteine residue, which subsequently undergoes carboxymethylation by the yeast ICMT Ste14 (added in excess to the reaction), using the radiolabeled methyl donor, [¹⁴C-methyl]-S-adenosyl methionine (SAM), provided in the reaction mix. The extent of carboxymethylation of the synthetic peptide is quantified using the vapor diffusion assay to measure the amount of base-labile [¹⁴C] methanol. The amount of methylation is quantified and, in turn, serves as an indirect proxy for the endoproteolytic activity of *ZMPSTE24*. This assay provides a robust and reliable

Table 1. C-terminal proteolytic activity of wild-type and mutant ZMPSTE24 proteins

ZMPSTE24	Specific activity ^a	% wild-type
WT	173.0 ± 6.2	100
H335A	0.7 ± 1.2	0.4
W340R	23.7 ± 1.4	13.7
P248L	7.9 ± 1.7	4.6
N265S	7.5 ± 1.5	4.3
L438F	1.8 ± 2.5	1.0
L94P	4.8 ± 1.6	2.8
W450X	0.6 ± 0.6	0.3
L362F(fsX18)	2.2 ± 0.5	1.3
T159_L209del	-2.7 ± 3.2	0

^aValues were derived from three separate experiments each performed in triplicate.

way to quantify ZMPSTE24 activity in a membrane preparation (53,57,59).

Using this coupled proteolysis assay, we measured the C-terminal proteolytic activity of yeast membranes containing wild-type ZMPSTE24, the null mutant H335A and the disease mutants. In nearly all cases, the membranes were prepared from the same strains as were used for the halo and mating assays above, which express ZMPSTE24 alleles on a *CEN* (single copy) plasmid. The L362F(fsX18) allele, which encodes a truncation product with 17 additional residues and is also referred to as Y379X, was expressed from a 2 μ m (multi-copy) plasmid, in an effort to determine whether any activity could be detected from the mutant protein. The specific activity calculated for each of the ZMPSTE24 alleles is indicated in Table 1 (middle column) and is displayed as a bar graph in Figure 4. The percentage of activity of each allele, normalized to wild-type ZMPSTE24, is also shown in Table 1 (right column).

The W340R point mutant retains the most activity of all the disease alleles, while P248L, N265S and L94P retain moderately less activity. The least activity is associated with the HEXXH domain mutant control (H335A) and the L438F, W450X, L362F(fsX18) and T159_L209del mutations. As evident by comparison of the graphs in Figures 3C and 4, the results from the activity assays are strikingly similar to those obtained with the quantitative mating assays. Notably, both assays indicate that the disease alleles fall into three groups: significant residual activity (W340R), some residual activity (P248L, N265S, L94P) and little or no residual activity (W450X, L362F(fsX18) and T159_L209del). The L438F allele demonstrates partial residual activity by mating, but virtually no enzyme activity. Immunoblotting of the membranes used for the activity assays (Fig. 5) revealed a varying amount of ZMPSTE24 protein in the membrane preparations (Fig. 5, see legend), which may indicate that certain disease mutations render the protein unstable. Changes in protein stability would not be unexpected, as several of the mutations are drastic, deleting large internal sections of the protein or eliminating the C-terminus. Interestingly, however, the expression and/or stability of the substitution mutations are also somewhat variable, possibly reflecting varying degrees of stability.

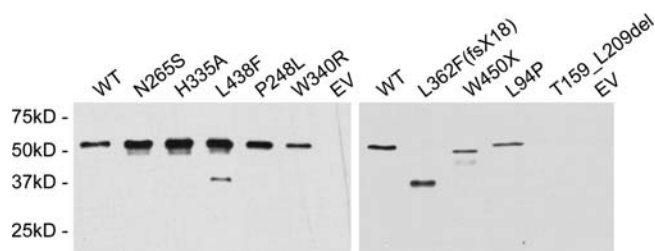


Figure 5. Expression of ZMPSTE24 mutant proteins when compared with the wild-type. Crude membranes prepared from yeast strains expressing WT and mutant His₁₀HA₃ ZMPSTE24, or empty vector (EV) were subjected to 10% SDS-PAGE, transferred to nitrocellulose membrane, probed with α -HA primary antibody and a goat α -mouse horseradish peroxidase-conjugated secondary antibody and detected by ECL. Varying amounts of crude membranes were added to each lane to optimize visualization of the signal. When compared with the WT, H335A catalytic site mutant, and most point mutants (left), the frameshift, deletion, nonsense and L94P mutations (right) required significantly more membranes for visualization. Amounts added to each lane are as follows: left panel: WT (0.5 μ g), N265S (0.5 μ g), H335A (0.5 μ g), L438F (0.5 μ g), P248L (1.0 μ g), W340R (3.0 μ g), EV (3.0 μ g); right panel: WT (0.1 μ g), L362F(fsX18) (2.0 μ g), W450X (3.0 μ g), L94P (12 μ g), T159_L209del (12 μ g) and EV (12 μ g).

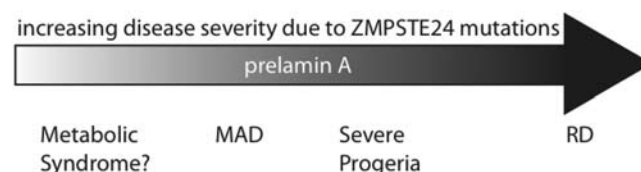


Figure 6. Schematic of the ZMPSTE24-associated progeroid disease severity spectrum. The results presented here and in other studies support the model that a spectrum of progeroid diseases of increasing severity, ranging from MAD-B to atypical progeria to RD, appears to correlate with an increasing amount of uncleaved prelamin A resulting from a failure of ZMPSTE24 cleavage. It has yet to be established whether metabolic syndrome is also directly connected to defects in prelamin A maturation, hence the question mark. The L438F studied here has been reported to be associated with metabolic syndrome (47), but the second patient allele is not known, and whether this mutation is truly causative of metabolic syndrome remains to be established.

DISCUSSION

The range of disease severity caused by mutations in ZMPSTE24 is quite broad, with the neonatal lethal disorder RD on one end of the spectrum, severe progeria (AT 'HGPS') characterized by a short lifespan midway through the spectrum and the relatively milder disease MAD-B, in which the lifespan of patients extends into the third decade or later, on the other end of the spectrum (Fig. 6) (27,29,38,43). It has been proposed that the greater the severity of disease, the lower the level of residual ZMPSTE24 activity that is retained (1,27–33). In this study, we have directly compared the activities of a number of disease alleles of ZMPSTE24 expressed in yeast, using quantitative mating and enzyme assays, as well as qualitative a-factor halo and mating assays. We wished to determine whether the disease severity spectrum shown in Figure 6 reflects the residual activity of ZMPSTE24 disease alleles.

Our results support the hypothesis that disease severity correlates with the cumulative, residual activity of ZMPSTE24 encoded by a patient's two alleles. For instance,

the combination of two alleles with molecular lesions predicted to be drastic, such as frameshifts, large internal deletions or early terminations, is associated with the lethal disease RD. Our studies confirm that the alleles L362F(fsX18) and T159_L209del show no residual activity. As can be seen in Figure 1, RD cases 10 and 16 are homozygous for these mutations, respectively. Therefore, RD appears to result when ZMPSTE24 activity is completely lacking. RD is lethal *in utero* or shortly after birth, representing an extreme example of the severity of defective ZMPSTE24 activity in which all of the lamin A present in patient cells is predicted to be in the persistently farnesylated, toxic form.

For the milder MAD-B disease (Fig. 1, lines 1–6), patient genotypes contain a null allele in combination with a substitution mutant (i.e. P248L, W340R, N265S) that has been predicted to retain partial function. Here, we provide evidence that these MAD-B alleles indeed show measurable residual activity, with W340R having significantly higher activity than others (Figs 3 and 4, and Table 1). One exception to the rule that MAD-B patients all have one complete null allele is shown in Figure 1, line 5, where the patient was homozygous for L94P (35). In this case, the L94P mutant would be predicted to be so minimally functional that even the two copies present in the patient would not suffice for normal function. Indeed, the L94P mutant is very severely reduced in activity in our assays (Figs 3 and 4, Table 1). Thus, the total enzymatic activity that the patient retained apparently fell below a critical threshold required for maintaining health and the absence of disease phenotypes. This mutant has been shown previously to cause prelamin A accumulation, and due to its location inside one of the transmembrane spans, was predicted to potentially interfere with membrane topology, such that the active site of ZMPSTE24 could be oriented on the inaccessible luminal side of the membrane (35). Taken together, our results suggest that most, if not all, MAD-B patients (Fig. 1, lines 1–7) must have at least one allele with residual activity. Thus, some, but not all, of the lamin A present in these MAD-B patient cells is predicted to be present in the aberrantly and persistently farnesylated form.

The range of diseases that are caused by mutations in ZMPSTE24 overlap in phenotype with HGPS, the classical premature aging disorder caused by mutations in *LMNA* that remove the ZMPSTE24 cleavage site in prelamin A through activation of a cryptic splice site (18–20). Somewhat confusingly, two cases of RD could also be attributed to mutations in the lamin A gene that are particularly robust activators of the cryptic splice site (22). The larger amount of progerin produced in these cases resulted in a disease that was phenotypically very similar to RD, but mapped to *LMNA* rather than *ZMPSTE24*. Conversely, a case of severe progeria was reported in which the patient had two null alleles of *ZMPSTE24* (Fig. 1, patient 9). This individual was shown to have a ‘mitigating’ mutation in one copy of the *LMNA* gene that resulted in 50% of the prelamin A being prematurely truncated prior to the CAAX motif (38). This *LMNA* mutation reduces the amount of uncleaved and persistently farnesylated prelamin A that the cells produce, and is thought to explain the severe progeria phenotype observed in the patient, rather than the RD phenotype that might be expected from the null *ZMPSTE24* genotype. Thus, the diagnosis of disease based

on the phenotype alone can be potentially misleading, and both genes, *ZMPSTE24* and *LMNA*, need to be examined for mutations. It is notable that there are two patients shown in Figure 1 (lines 6 and 8) that have the identical *ZMPSTE24* genotypes (N265S and L362F(fsX18)), but different diseases, namely MAD-B and atypical progeria, respectively. It is possible that additional modifier genes, still unaccounted for, may also contribute to the severity of these progeroid diseases.

Metabolic syndrome, which encompasses several risk factors for cardiovascular disease, is often present in MAD patients (60). Interestingly, the heterozygous L438F mutation was found in a patient presenting only with metabolic syndrome (47). As the genetics of the *ZMPSTE24* diseases would indicate that haploinsufficiency is not normally causative of disease, this is an unusual case. It should be noted that another case of heterozygosity in a patient with MAD has been reported (Fig. 1, case 7); however, the authors suggested that although a second mutation was not identified, it may nevertheless indeed be present, especially since the heterozygous parents of the patient were reported as phenotypically normal (37).

The methods of analysis presented in this study, involving expression of *ZMPSTE24* disease alleles in yeast, combined with the performance of several simple quantitative assays, provides the basis for assessing new disease alleles that may be discovered in the future. Such information will be useful for future studies directed toward dissecting the enzymatic mechanism of proteolysis, which to date remains unknown. Interestingly, several lines of study have suggested that an understanding of the mechanism could be critical for predicting (and preventing) potential off-target drug effects. For instance, drug cocktails used to treat patients infected with HIV have often included aspartyl protease inhibitors, some of which have been experimentally demonstrated to inhibit ZMPSTE24 activity *in vitro* and *in vivo* (57,58). It remains unclear whether the side effects exhibited by patients who have spent decades on these drugs (which include lipodystrophies, metabolic disorders and premature aging) are indeed attributable to the inhibition of ZMPSTE24. It is also worthwhile to note that the down-regulation of *ZMPSTE24* expression has been associated with normal physiological aging (61). Further work on the activity and regulation of ZMPSTE24 will be needed to fully probe these potentially important connections.

MATERIALS AND METHODS

Plasmid constructs

The experiments in this study were carried out using *CEN URA3* yeast plasmid constructs expressed in the strain SM3614 (*MATa ste24Δ rce1Δ*). These plasmids encode an *N*-terminally His₁₀HA₃-tagged version of human ZMPSTE24 expressed from a PGK promoter with the following mutations: WT (pSM2677), P248L (pSM2676), H335A (pSM2673), W340R (pSM2672), N265S (pSM2671), T159_L209del (pSM2670), L362F(fsX18) (pSM2669), L94P (pSM2678), L438F (pSM2680) and W450X (pSM2679). These constructs were made as described below.

Constructs used to express human *ZMPSTE24* and individual disease mutations were first created in a yeast $2\ \mu\text{m}$ *URA3* vector backbone. The method of homologous recombination of overlapping PCR and vector products in *S. cerevisiae* was used to introduce mutations. Plasmids were rescued from yeast and transformed into the recombination deficient STBL2 *E. coli* strain (Invitrogen). The base plasmid pSM1282 (17) containing the yeast *STE24* gene with an N-terminal HIS-HA tag ($\text{His}_{10}\text{HA}_3$) under the control of the PGK promoter was gapped by removal of the *ySTE24* ORF and used as the vector backbone for all homologous recombination reactions. PCR products containing the entire ORF of wild-type or mutant *ZMPSTE24* alleles with overlapping homologous 5' and 3' ends and gapped pSM1282 were co-transformed into the yeast strain SM3103 (*trp1 leu2 ura3 his4 can1 ste24::LEU2*) (48). It is important to note that bacteria-containing *ZMPSTE24* plasmids were propagated on selective media at 25°C. The use of STBL2 bacterial cells and low temperature was necessary to prevent toxicity and/or recombination and rearrangement events in *E. coli*. Such events occur frequently for *ZMPSTE24* in bacteria when these conditions are not used. Plasmids were purified and sequenced to ensure that the desired mutation was obtained. The wild-type and *ZMPSTE24* mutant alleles were subsequently transferred to a *CEN URA3* vector (pRS316), using standard restriction digestion/ligation-mediated cloning techniques.

All plasmids and strains used in this study are freely available upon request.

Halo and mating assays

Halo assays were performed essentially as previously described (49,51,54,56). Briefly, yeast strains (SM3614, *MATa ste24Δ rce1Δ*) expressing wild-type or mutant *ZMPSTE24* on the *CEN URA3* plasmid (see above) were grown overnight in selective (SC-URA) media, concentrated by centrifugation and resuspended in sterile water. The yeast strains used were as follows: WT (SM5973), P248L (SM5978), H335A (SM5975), W340R (SM5977), N265S (SM5974), T159_L209del (SM5976), L362F(fsX18) (SM5981), L94P (SM5983), L438F (SM5985) and W450X (SM5984). Five microliters of each strain was spotted onto a lawn of the halo tester SM2375 (*MATa sst2*) mutant yeast cells spread on YPD plates containing 0.04% Triton X-100. Inclusion of TX-100 in the plates allows and even diffusion of a-factor and a sharper halo. Plates were incubated at 30°C for 2 days.

The qualitative spot-mating assay was performed essentially as described previously (49,51,54,56). Briefly, overnight cultures (SC-URA) of the *MATa* yeast strains expressing wild-type *ZMPSTE24* or the mutant alleles (described above) were diluted to OD_{600} of 1.0 in sterile water. Ten microliters of each strain was spotted onto a lawn of *MATa far1* mating tester strain (SM2882) spread on synthetic medium (SD) to select for diploids. Plates were incubated at 30°C for 2 days.

Quantitative mating assays were performed essentially as described previously (49,51,54,56), except that a *far1* strain was used as a mating partner (55). Briefly, overnight cultures of the yeast strains expressing wild-type *ZMPSTE24* or mutant alleles (described above) were diluted to OD_{600} 1 in sterile

water. Equal volumes (0.5 ml) of the tester strain (*MATa far1*) and each of the strains expressing *ZMPSTE24* alleles were mixed and applied to a nitrocellulose filter, excess liquid was removed by applying a vacuum and the filters were placed on a YPD plate. Plates were incubated at 30°C for 4 h to allow mating to occur. Cells were washed off of the filters by vortexing in sterile water, and serial 10-fold dilutions were prepared and plated on diploid-selective plates (SD) or non-selective plates (YPD). The mating efficiency for each of the strains tested was calculated as the ratio of diploids to total cells, and graphed as a percentage of the mating efficiency of the yeast strain expressing wild-type *ZMPSTE24*. Mating tests were performed in triplicate and the error bars indicate standard deviation.

ZMPSTE24 *in vitro* assay

Human *ZMPSTE24* activity was determined using a radioactive *in vitro*-coupled proteolysis and methyltransferase vapor diffusion assay as described previously (57), with minor modifications. Briefly, the human wild-type and mutant *ZMPSTE24* variants used for the mating and halo tests above, or the yeast Ste14p-isoprenylcysteine carboxyl methyltransferase (ICMT), were expressed in the SM3614 ($\Delta\text{ste24}\Delta\text{rce1}$) yeast strain and the membrane fractions were isolated as described previously (59). It should be noted that mutant L362F(fsX18) was expressed from a high copy ($2\ \mu$) yeast plasmid, rather than a low copy *CEN* plasmid for the *in vitro* assay and immunoblot (Figs 4 and 5, and Table 1). Reaction mixtures contained 5 μg of membranes expressing *ZMPSTE24* or its variants, an excess (8 μg) of membranes expressing Ste14p, 25 μM farnesylated a-factor peptide (YIIKGVFWDPA-farnCVIA) (EZ Biolabs), and 20 μM S-adenosyl [^{14}C -methyl]-L-methionine in 100 mM Tris-HCl (pH 7.5) in a total volume of 60 μl . The reaction mixtures were incubated at 30°C for 30 min and quenched by the addition of 50 μl 1 M NaOH/1% SDS. The reaction mixture (100 μl) was spotted onto pleated filter and placed in the neck of a scintillation vial containing 10 ml of Biosafe II scintillation fluid (RPI, Mount Prospect, IL, USA) and capped. The [^{14}C]methanol released from the cleaved and methylated substrate as a result of quenching the reaction was allowed to diffuse into the scintillation fluid for 2.5 h at room temperature. The filter paper was then removed and the radioactivity was quantified by scintillation counting. Specific activity was reported as pmol of VIA groups removed/min/mg *ZMPSTE24*, as measured by the methyltransferase assay. Each value was derived from three assays performed in triplicate.

Immunoblotting and antibodies

Crude membranes prepared from yeast strains expressing wild-type and mutant $\text{His}_{10}\text{HA}_3$ -N-terminally tagged *ZMPSTE24* were heated at 65°C for 30 min in $2\times$ SDS. The samples were subjected to SDS-PAGE (10% gel) and transferred to a 0.2 μm nitrocellulose membrane. The nitrocellulose membrane was blocked overnight in 20% non-fat dry milk. *ZMPSTE24* was detected with the α -HA primary antibody (1:15,000) and goat α -mouse horseradish peroxidase-

conjugated secondary antibody (1:4,000), using enhanced chemiluminescence (ECL) to visualize the signal (Pierce SuperSignal West Pico Chemiluminescent Substrate).

SUPPLEMENTARY MATERIAL

Supplementary Material is available at *HMG* online.

ACKNOWLEDGEMENTS

We thank Megan Kane for critical comments on this manuscript

Conflict of Interest: The authors declare no conflict of interest.

FUNDING

This work was supported by the National Institutes of Health (grant number RO1 GM41223 to S.M.).

REFERENCES

- Barrowman, J. and Michaelis, S. (2009) ZMPSTE24, an integral membrane zinc metalloprotease with a connection to progeroid disorders. *Biol. Chem.*, **390**, 761–773.
- Bergo, M.O., Gavino, B., Ross, J., Schmidt, W.K., Hong, C., Kendall, L.V., Mohr, A., Meta, M., Genant, H., Jiang, Y. *et al.* (2002) Zmpste24 deficiency in mice causes spontaneous bone fractures, muscle weakness, and a prelamin A processing defect. *Proc. Natl Acad. Sci. USA*, **99**, 13049–13054.
- Pendas, A.M., Zhou, Z., Cadinanos, J., Freije, J.M., Wang, J., Hultenby, K., Astudillo, A., Wernerson, A., Rodriguez, F., Tryggvason, K. *et al.* (2002) Defective prelamin A processing and muscular and adipocyte alterations in Zmpste24 metalloproteinase-deficient mice. *Nat. Genet.*, **31**, 94–99.
- Young, S.G., Fong, L.G. and Michaelis, S. (2005) Prelamin A, Zmpste24, misshapen cell nuclei, and progeria—new evidence suggesting that protein farnesylation could be important for disease pathogenesis. *J. Lipid Res.*, **46**, 2531–2558.
- Dittmer, T.A. and Misteli, T. (2011) The lamin protein family. *Genome Biol.*, **12**, 222.
- Gruenbaum, Y., Margalit, A., Goldman, R.D., Shumaker, D.K. and Wilson, K.L. (2005) The nuclear lamina comes of age. *Nat. Rev. Mol. Cell Biol.*, **6**, 21–31.
- Mattout, A., Dechat, T., Adam, S.A., Goldman, R.D. and Gruenbaum, Y. (2006) Nuclear lamins, diseases and aging. *Curr. Opin. Cell Biol.*, **18**, 335–341.
- Worman, H.J. and Bonne, G. (2007) ‘Laminopathies’: a wide spectrum of human diseases. *Exp. Cell Res.*, **313**, 2121–2133.
- Wright, L.P. and Philips, M.R. (2006) Thematic review series: lipid posttranslational modifications. CAAX modification and membrane targeting of Ras. *J. Lipid Res.*, **47**, 883–891.
- Beck, L.A., Hosick, T.J. and Sinensky, M. (1990) Isoprenylation is required for the processing of the lamin A precursor. *J. Cell Biol.*, **110**, 1489–1499.
- Weber, K., Plessmann, U. and Traub, P. (1989) Maturation of nuclear lamin A involves a specific carboxy-terminal trimming, which removes the polyisoprenylation site from the precursor; implications for the structure of the nuclear lamina. *FEBS Lett.*, **257**, 411–414.
- Davies, B.S., Fong, L.G., Yang, S.H., Coffinier, C. and Young, S.G. (2009) The posttranslational processing of prelamin A and disease. *Annu. Rev. Genomics Hum. Genet.*, **10**, 153–174.
- Barrowman, J., Hamblet, C., Kane, M.S. and Michaelis, S. (2012) Requirements for efficient proteolytic cleavage of prelamin A by ZMPSTE24. *PLoS ONE*, **7**, e32120.
- Barrowman, J., Hamblet, C., George, C.M. and Michaelis, S. (2008) Analysis of prelamin A biogenesis reveals the nucleus to be a CaaX processing compartment. *Mol. Biol. Cell*, **19**, 5398–5408.
- Schmidt, W.K., Tam, A., Fujimura-Kamada, K. and Michaelis, S. (1998) Endoplasmic reticulum membrane localization of Rce1p and Ste24p, yeast proteases involved in carboxyl-terminal CAAX protein processing and amino-terminal a-factor cleavage. *Proc. Natl Acad. Sci. USA*, **95**, 11175–11180.
- Tam, A., Nouvet, F.J., Fujimura-Kamada, K., Slunt, H., Sisodia, S.S. and Michaelis, S. (1998) Dual roles for Ste24p in yeast a-factor maturation: NH₂-terminal proteolysis and COOH-terminal CAAX processing. *J. Cell Biol.*, **142**, 635–649.
- Tam, A., Schmidt, W.K. and Michaelis, S. (2001) The multispanning membrane protein Ste24p catalyzes CAAX proteolysis and NH₂-terminal processing of the yeast a-factor precursor. *J. Biol. Chem.*, **276**, 46798–46806.
- De Sandre-Giovannoli, A. and Levy, N. (2006) Altered splicing in prelamin A-associated premature aging phenotypes. *Prog. Mol. Subcell. Biol.*, **44**, 199–232.
- Eriksson, M., Brown, W.T., Gordon, L.B., Glynn, M.W., Singer, J., Scott, L., Erdos, M.R., Robbins, C.M., Moses, T.Y., Berglund, P. *et al.* (2003) Recurrent de novo point mutations in lamin A cause Hutchinson–Gilford progeria syndrome. *Nature*, **423**, 293–298.
- Merideth, M.A., Gordon, L.B., Clauss, S., Sachdev, V., Smith, A.C., Perry, M.B., Brewer, C.C., Zalewski, C., Kim, H.J., Solomon, B. *et al.* (2008) Phenotype and course of Hutchinson–Gilford progeria syndrome. *N. Engl. J. Med.*, **358**, 592–604.
- Scaffidi, P., Gordon, L. and Misteli, T. (2005) The cell nucleus and aging: tantalizing clues and hopeful promises. *PLoS Biol.*, **3**, e395.
- Moulson, C.L., Fong, L.G., Gardner, J.M., Farber, E.A., Go, G., Passariello, A., Grange, D.K., Young, S.G. and Miner, J.H. (2007) Increased progerin expression associated with unusual LMNA mutations causes severe progeroid syndromes. *Hum. Mutat.*, **28**, 882–889.
- Fong, L.G., Frost, D., Meta, M., Qiao, X., Yang, S.H., Coffinier, C. and Young, S.G. (2006) A protein farnesyltransferase inhibitor ameliorates disease in a mouse model of progeria. *Science*, **311**, 1621–1623.
- Yang, S.H., Chang, S.Y., Ren, S., Wang, Y., Andres, D.A., Spielmann, H.P., Fong, L.G. and Young, S.G. (2011) Absence of progeria-like disease phenotypes in knock-in mice expressing a non-farnesylated version of progerin. *Hum. Mol. Genet.*, **20**, 436–444.
- Capell, B.C., Olive, M., Erdos, M.R., Cao, K., Faddah, D.A., Tavarez, U.L., Conneely, K.N., Qu, X., San, H., Ganesh, S.K. *et al.* (2008) A farnesyltransferase inhibitor prevents both the onset and late progression of cardiovascular disease in a progeria mouse model. *Proc. Natl Acad. Sci. USA*, **105**, 15902–15907.
- Fong, L.G., Ng, J.K., Meta, M., Cote, N., Yang, S.H., Stewart, C.L., Sullivan, T., Burghardt, A., Majumdar, S., Reue, K. *et al.* (2004) Heterozygosity for Lmna deficiency eliminates the progeria-like phenotypes in Zmpste24-deficient mice. *Proc. Natl Acad. Sci. USA*, **101**, 18111–18116.
- Agarwal, A.K., Fryns, J.P., Auchus, R.J. and Garg, A. (2003) Zinc metalloproteinase, ZMPSTE24, is mutated in mandibuloacral dysplasia. *Hum. Mol. Genet.*, **12**, 1995–2001.
- Miyoshi, Y., Akagi, M., Agarwal, A.K., Namba, N., Kato-Nishimura, K., Mohri, I., Yamagata, M., Nakajima, S., Mushiaki, S., Shima, M. *et al.* (2008) Severe mandibuloacral dysplasia caused by novel compound heterozygous ZMPSTE24 mutations in two Japanese siblings. *Clin. Genet.*, **73**, 535–544.
- Moulson, C.L., Go, G., Gardner, J.M., van der Wal, A.C., Smitt, J.H., van Hagen, J.M. and Miner, J.H. (2005) Homozygous and compound heterozygous mutations in ZMPSTE24 cause the laminopathy restrictive dermopathy. *J. Invest. Dermatol.*, **125**, 913–919.
- Smigiel, R., Jakubiak, A., Esteves-Vieira, V., Szela, K., Halon, A., Jurek, T., Levy, N. and De Sandre-Giovannoli, A. (2010) Novel frameshifting mutations of the ZMPSTE24 gene in two siblings affected with restrictive dermopathy and review of the mutations described in the literature. *Am. J. Med. Genet. A*, **152A**, 447–452.
- Varela, I., Cadinanos, J., Pendas, A.M., Gutierrez-Fernandez, A., Folgueras, A.R., Sanchez, L.M., Zhou, Z., Rodriguez, F.J., Stewart, C.L., Vega, J.A. *et al.* (2005) Accelerated ageing in mice deficient in Zmpste24 protease is linked to p53 signalling activation. *Nature*, **437**, 564–568.

32. Ahmad, Z., Zackai, E., Medne, L. and Garg, A. (2010) Early onset mandibuloacral dysplasia due to compound heterozygous mutations in ZMPSTE24. *Am. J. Med. Genet. A*, **152A**, 2703–2710.
33. Shackleton, S., Smallwood, D.T., Clayton, P., Wilson, L.C., Agarwal, A.K., Garg, A. and Trembath, R.C. (2005) Compound heterozygous ZMPSTE24 mutations reduce prelamin A processing and result in a severe progeroid phenotype. *J. Med. Genet.*, **42**, e36.
34. Agarwal, A.K., Zhou, X.J., Hall, R.K., Nicholls, K., Bankier, A., Van Esch, H., Fryns, J.P. and Garg, A. (2006) Focal segmental glomerulosclerosis in patients with mandibuloacral dysplasia owing to ZMPSTE24 deficiency. *J. Investig. Med.*, **54**, 208–213.
35. Ben Yaou, R., Navarro, C., Quijano-Roy, S., Bertrand, A.T., Massart, C., De Sandre-Giovannoli, A., Cadinanos, J., Mamchaoui, K., Butler-Browne, G., Estournet, B. *et al.* (2011) Type B mandibuloacral dysplasia with congenital myopathy due to homozygous ZMPSTE24 missense mutation. *Eur. J. Hum. Genet.*, **19**, 647–654.
36. Cunningham, V.J., D'Apice, M.R., Licata, N., Novelli, G. and Cundy, T. (2010) Skeletal phenotype of mandibuloacral dysplasia associated with mutations in ZMPSTE24. *Bone*, **47**, 591–597.
37. Thill, M., Nguyen, T.D., Wehnert, M., Fischer, D., Hausser, I., Braun, S. and Jackisch, C. (2008) Restrictive dermopathy: a rare laminopathy. *Arch. Gynecol. Obstet.*, **278**, 201–208.
38. Denecke, J., Brune, T., Feldhaus, T., Robenek, H., Kranz, C., Auchus, R.J., Agarwal, A.K. and Marquardt, T. (2006) A homozygous ZMPSTE24 null mutation in combination with a heterozygous mutation in the LMNA gene causes Hutchinson-Gilford progeria syndrome (HGPS): insights into the pathophysiology of HGPS. *Hum. Mutat.*, **27**, 524–531.
39. Chen, M., Kuo, H.H., Huang, Y.C., Ke, Y.Y., Chang, S.P., Chen, C.P., Lee, D.J., Lee, M.L., Lee, M.H., Chen, T.H. *et al.* (2009) A case of restrictive dermopathy with complete chorioamniotic membrane separation caused by a novel homozygous nonsense mutation in the ZMPSTE24 gene. *Am. J. Med. Genet. A*, **149A**, 1550–1554.
40. Jagadeesh, S., Bhat, L., Suresh, I. and Muralidhar, S.L. (2009) Prenatal diagnosis of restrictive dermopathy. *Indian Pediatr.*, **46**, 349–351.
41. Kariminejad, A., Goodarzi, P., Thanh Huong le, T. and Wehnert, M.S. (2009) Restrictive dermopathy. Molecular diagnosis of restrictive dermopathy in a stillborn fetus from a consanguineous Iranian family. *Saudi Med. J.*, **30**, 150–153.
42. Morais, P., Magina, S., Ribeiro, M.D., Rodrigues, M., Lopes, J.M., Thanh, H.L., Wehnert, M. and Guimaraes, H. (2008) Restrictive dermopathy—a lethal congenital laminopathy. Case report and review of the literature. *Eur. J. Pediatr.*, published online, doi:10.1007/s00431-00008-00868-x.
43. Navarro, C.L., Cadinanos, J., De Sandre-Giovannoli, A., Bernard, R., Courrier, S., Boccaccio, I., Boyer, A., Kleijer, W.J., Wagner, A., Giuliano, F. *et al.* (2005) Loss of ZMPSTE24 (FACE-1) causes autosomal recessive restrictive dermopathy and accumulation of Lamin A precursors. *Hum. Mol. Genet.*, **14**, 1503–1513.
44. Sander, C.S., Salman, N., van Geel, M., Broers, J.L., Al-Rahmani, A., Chedid, F., Hausser, I., Oji, V., Al Nuaimi, K., Berger, T.G. *et al.* (2008) A newly identified splice site mutation in ZMPSTE24 causes restrictive dermopathy in the Middle East. *Br. J. Dermatol.*, **159**, 961–967.
45. Navarro, C.L., De Sandre-Giovannoli, A., Bernard, R., Boccaccio, I., Boyer, A., Genevieve, D., Hadj-Rabia, S., Gaudy-Marqueste, C., Smitt, H.S., Vabres, P. *et al.* (2004) Lamin A and ZMPSTE24 (FACE-1) defects cause nuclear disorganization and identify restrictive dermopathy as a lethal neonatal laminopathy. *Hum. Mol. Genet.*, **13**, 2493–2503.
46. Agarwal, A.K. and Garg, A. (2006) Genetic disorders of adipose tissue development, differentiation, and death. *Annu. Rev. Genomics Hum. Genet.*, **7**, 175–199.
47. Dutour, A., Roll, P., Gaborit, B., Courrier, S., Alessi, M.C., Tregouet, D.A., Angelis, F., Robaglia-Schlupp, A., Lesavre, N., Cau, P. *et al.* (2011) High prevalence of laminopathies among patients with metabolic syndrome. *Hum. Mol. Genet.*, **20**, 3779–3786.
48. Fujimura-Kamada, K., Nouvet, F.J. and Michaelis, S. (1997) A novel membrane-associated metalloprotease, Ste24p, is required for the first step of NH2-terminal processing of the yeast a-factor precursor. *J. Cell Biol.*, **136**, 271–285.
49. Barrowman, J. and Michaelis, S. (2011) Hrycyna, C.A., Bergo, M.O. and Tamanoi, F. (eds), In *The Enzymes*. Academic Press, Burlington, Vol. 30, pp. 13–41.
50. Boyartchuk, V.L. and Rine, J. (1998) Roles of prenyl protein proteases in maturation of *Saccharomyces cerevisiae* a-factor. *Genetics*, **150**, 95–101.
51. Huyer, G., Kistler, A., Nouvet, F.J., George, C.M., Boyle, M.L. and Michaelis, S. (2006) *Saccharomyces cerevisiae* a-factor mutants reveal residues critical for processing, activity, and export. *Eukaryot. Cell*, **5**, 1560–1570.
52. Schmidt, W.K., Tam, A. and Michaelis, S. (2000) Reconstitution of the Ste24p-dependent N-terminal proteolytic step in yeast a-factor biogenesis. *J. Biol. Chem.*, **275**, 6227–6233.
53. Leung, G.K., Schmidt, W.K., Bergo, M.O., Gavino, B., Wong, D.H., Tam, A., Ashby, M.N., Michaelis, S. and Young, S.G. (2001) Biochemical studies of Zmpste24-deficient mice. *J. Biol. Chem.*, **276**, 29051–29058.
54. Nijbroek, G.L. and Michaelis, S. (1998) Functional assays for analysis of yeast ste6 mutants. *Methods Enzymol.*, **292**, 193–212.
55. Peter, M. and Herskowitz, I. (1994) Direct inhibition of the yeast cyclin-dependent kinase Cdc28-Cln by Far1. *Science*, **265**, 1228–1231.
56. Berkower, C. and Michaelis, S. (1991) Mutational analysis of the yeast a-factor transporter STE6, a member of the ATP binding cassette (ABC) protein superfamily. *EMBO J.*, **10**, 3777–3785.
57. Coffinier, C., Hudon, S.E., Farber, E.A., Chang, S.Y., Hrycyna, C.A., Young, S.G. and Fong, L.G. (2007) HIV protease inhibitors block the zinc metalloproteinase ZMPSTE24 and lead to an accumulation of prelamin A in cells. *Proc. Natl Acad. Sci. USA*, **104**, 13432–13437.
58. Hudon, S.E., Coffinier, C., Michaelis, S., Fong, L.G., Young, S.G. and Hrycyna, C.A. (2008) HIV-protease inhibitors block the enzymatic activity of purified Ste24p. *Biochem. Biophys. Res. Commun.*, **374**, 365–368.
59. Anderson, J.L., Frase, H., Michaelis, S. and Hrycyna, C.A. (2005) Purification, functional reconstitution, and characterization of the *Saccharomyces cerevisiae* isoprenylcysteine carboxylmethyltransferase Ste14p. *J. Biol. Chem.*, **280**, 7336–7345.
60. Agarwal, A.K. and Garg, A. (2006) Genetic basis of lipodystrophies and management of metabolic complications. *Annu. Rev. Med.*, **57**, 297–311.
61. Ragnauth, C.D., Warren, D.T., Liu, Y., McNair, R., Tajsic, T., Figg, N., Shroff, R., Skepper, J. and Shanahan, C.M. (2010) Prelamin A acts to accelerate smooth muscle cell senescence and is a novel biomarker of human vascular aging. *Circulation*, **121**, 2200–2210.